JCIM JOURNAL OF CHEMICAL INFORMATION AND MODELING

Cite This: J. Chem. Inf. Model. XXXX, XXX, XXX−XXX

Article

pubs.acs.org/jcim

A Molecular Dynamics Investigation of the Thermostability of Cold-Sensitive I707L KlenTaq1 DNA Polymerase and Its Wild-Type Counterpart

Erica Modeste,[†] Lily Mawby,[†] Bill Miller, III,[‡] Eugene Wu,[§] and Carol A. Parish*[,†]

[†]Department of Chemistry, Gottwald Center for the Sciences, University of Richmond, Richmond, Virginia 23713, United States

[‡]Department of Chemistry, Truman State University, Kirksville, Missouri 63501, United States

[§]Department of Biology, Gottwald Center for the Sciences, University of Richmond, Richmond, Virginia 23713, United States

Supporting Information

ABSTRACT: DNA polymerase I from *Thermus aquaticus* (*Taq* DNA polymerase) is useful for polymerase chain reactions because of its exceptional thermostability; however, its activity at low temperatures can cause amplification of unintended products. Mutation of isoleucine 707 to leucine (I707L) slows *Taq* DNA polymerase at low temperatures, which decreases unwanted amplification due to mispriming. In this work, unrestrained molecular dynamics (MD) simulations were performed on I707L and wild-type (WT) *Taq* DNA polymerase at 341 and 298 K to determine how the mutation affects the dynamic nature of the protein. The results suggest that I707L *Taq* DNA polymerase remains relatively immobile at room temperature and becomes more flexible at the higher temperature, while the WT *Taq* DNA polymerase demonstrates less substantial differences in dynamics at high and low temperatures. These results are in agreement with previous experimental results on the I707L mutant *Taq* DNA polymerase that show dynamic differences at high and low temperatures. The decreased mobility of the mutant at low temperature suggests that the mutant remains longer in the blocked conformation, and this may lead to reduced activity relative to the WT at 298 K. Principal component analysis revealed that the mutation results in decoupled movements of the Q helix and fingers domain. This decoupled nature of the mutant gives way to an increasingly flexible N-terminal end of the Q helix at 341 K, a characteristic not seen for WT *Taq* DNA polymerase.

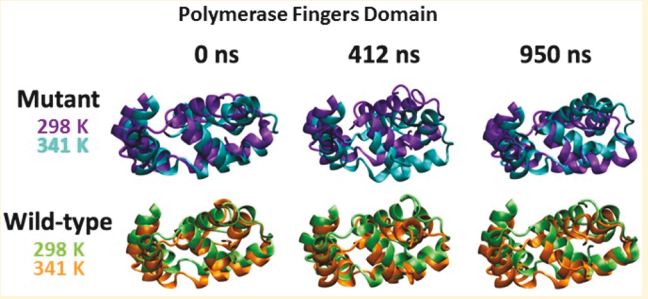

INTRODUCTION

DNA polymerase plays an essential role in the important biological technique of polymerase chain reaction (PCR). DNA polymerase I from *Thermus aquaticus* (*Taq* DNA polymerase) is an ideal prototype for PCR because of its thermostability and activity at high temperatures.[1] Despite the ability of *Taq* DNA polymerase to function at high temperatures, it also exhibits substantial activity at room temperature. At temperatures below the primer annealing temperature, oligonucleotides often bind to sites that are not perfect reverse complements of their sequences. DNA polymerase activity then results in the production of misprimed and nonspecific products.[2] Mispriming is a consequence of DNA synthesis occurring before the PCR reaction has reached the optimal operating temperature. One approach to prevent the formation of such unwanted misprimed products is to reduce or prevent DNA synthesis below typical primer annealing temperatures of 50−60 °C.

Kermekchiev and colleagues[3] sought to reduce unwanted products at low temperatures by identifying mutants of *Taq* DNA polymerase that had suppressed activity at 37 °C and high activity at 68 °C. After conducting a series of mutations throughout the large (5′-to-3′ exonuclease-deleted) fragment of *Taq* DNA polymerase, they were able to identify four cold-sensitive mutants (E626K, W706R, I707L, and E708D) that contained residue modifications in the P α-helix (Figure 1A), located on the outside surface of the fingers domain. The P helix is located at a fulcrum that is believed to function by exerting pressure on the neighboring Q helix, conceivably magnifying the structural or dynamical effects of the fingers domain.[4,5] Another study showed that a G850R mutation in the Q helix of *Escherichia coli* DNA polymerase caused the enzyme to be less processive, pointing to the importance of the Q helix in the function of the polymerase.[5]

One mutation of particular interest is a conservative mutation at residue 707 from an isoleucine to a leucine.[3] The experimental structure of this mutant showed that the fingers domain and the DNA strand undergo major conformational changes relative to the wild-type (WT) structure.[4] The isoleucine to leucine mutation in the P helix of *Taq* DNA polymerase allows a

Special Issue: Women in Computational Chemistry

Received: January 5, 2019
Published: March 21, 2019

DOI: 10.1021/acs.jcim.9b00022
J. Chem. Inf. Model. XXXX, XXX, XXX−XXX

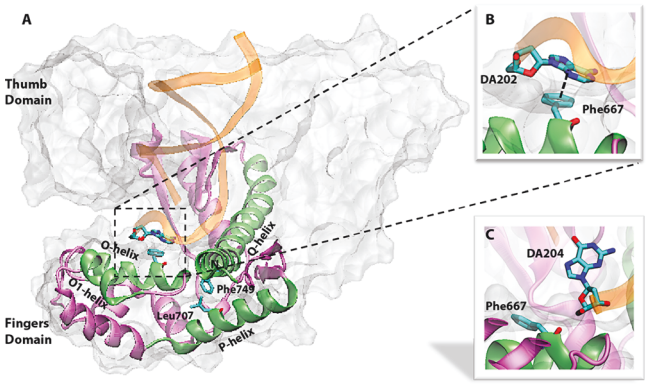

Figure 1. (A) Schematic diagram of I707L *Taq* DNA polymerase bound to DNA in the blocked position, with key residues Leu707, Phe749, Phe667, and DA202 highlighted. The DNA strand is shown as a flat tan ribbon. (B) π stacking between Phe667 and DA202 sustains the positioning of the template DNA strand in the blocked position. (C) In the unblocked position, the bottom single-stranded template base nucleotide, DA204, is flipped out of the stacking arrangement.

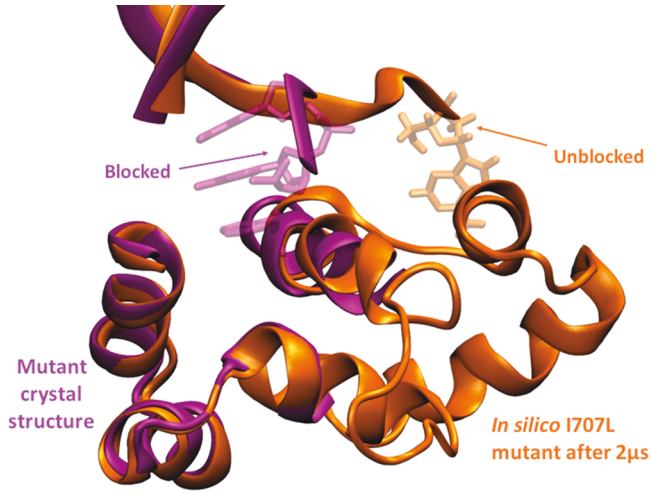

Figure 2. Overlay of the tip of the fingers domain in the mutant crystal structure (purple, PDB code 4N56) and the in silico I707L mutant after 2 μs of simulation (orange). The orange arrow points to the positioning of the template strand in the unblocked position, while the purple arrow points to the positioning of the template strand in the blocked position. Close alignment of residues between the experimental (4N56) and simulated structures suggests that the fingers domain in the simulated structure has adopted the proper conformation to be used to model residues missing from the experimental structure (the missing experimental fingers domain is the missing purple region in the lower-right corner of the image).

neighboring phenylalanine (Phe749), located on the Q helix, to adopt an alternate conformation, vacating space in the fingers subdomain (Figure 1A). This space can then be filled by movements of the O helix, the O1 helix, and the loop between the two helices. This chain reaction of small movements gives way to an active-site cleft large enough to be occupied by stacked nucleotides from the template overhang, blocking the polymerase active site. Electrostatic surface maps comparing the WT and mutant experimental structures highlight these changes (Figure S1). This is the atomistic picture that unfolds from an examination of the static experimental structures, but to our knowledge there has been no dynamical investigation of the role of this single-point mutation on the polymerase mechanism of action.

When the polymerase active site is blocked, nucleotide incorporation cannot occur because the template DNA strand is positioned within the active site, blocking the nucleotide binding site (Figure 2). In the mutant binary structure (PDB code 4N56), the template DNA strand is in alignment with the rest of the duplex DNA (Figure 1A), and its position is maintained in the blocked position by π-stacking interactions between the first unpaired base of the template strand, DA202, and Phe667 (Figure 1B).[4] The DNA strand in the unblocked position is characterized by the DNA template strand sitting outside the active site (Figure 2) in a position where it does not interfere with nucleotide incorporation (PDB code 4KTQ). In this case, the first single-stranded template base is flipped out of the stacking arrangement of the duplex DNA (Figure 1C), resting within the crevice of the thumb and fingers domains.[6]

Reorganization of the fingers domain and template DNA strand supports the hypothesis that the conservative I707L mutation is located at a fulcrum that has large, long-range effects. However, it remains unclear how this mutation and the corresponding structural changes alter the dynamical behavior of the polymerase over long distances. Thus, we utilized unrestrained (unbiased) molecular dynamics (MD) simulations to yield insight into how the mutation affects the dynamics of the protein at low and high temperatures.

METHODS

Preparation of Initial Structures for Molecular Dynamics Simulations. There are five binary (enzyme:DNA) Klen Taq1 DNA polymerase (KlenTaq1) experimental structures available in the Protein Data Bank: 4N56,[4] 4KTQ,[6] 3SZ2, 3SV4, and 3SYZ.[7] KlenTaq1 is a deletion mutant of *Taq* DNA polymerase missing the N-terminal 5′-to-3′ exonuclease domain, which is not essential for nucleotide polymerization activity.[5,6] In a binary structure, the DNA template strand can adopt either a blocked or unblocked orientation relative to the active site. The blocked position has the template strand sitting directly over the active site and blocking the insertion of an incoming nucleotide. The unblocked orientation has the DNA template strand rotated away from the active site (Figures 1 and 2).[4] The blocked/unblocked nomenclature is distinct from the open/closed notation. In a binary open structure, the tip of the fingers domain is rotated away from the active site. In the ternary complex, nucleotide binding causes a transition in the fingers domain from the open to the closed conformation. The conversion from open to closed rotates the fingers domain toward the active site by approximately 46°.[6] Previous work using *Bacillus stearothermophilus* DNA polymerase showed that the dominant binary conformation is the open orientation.[8] The 4KTQ binary experimental structure is a wild-type (WT) polymerase with the template strand in the unblocked position and the fingers domain in the open position. The 4N56 structure is a binary I707L polymerase mutant with the DNA strand in the blocked position. The 4N56 structure is missing residues 643−660 and 673−699 from the fingers domain. 3SYZ is a binary WT with the DNA template strand in the blocked position. The fingers domain in this structure is not well-resolved, as suggested by the high *B*-factor values associated with residues 644−659 and 677−688.[7] It is not uncommon to see high *B*-factor values

DOI: 10.1021/acs.jcim.9b00022
J. Chem. Inf. Model. XXXX, XXX, XXX−XXX

caused by the corresponding disorder present in proteins that interact with DNA.[9]

To build the mutant blocked structure, we started from the 4N56 binary mutant structure in the blocked orientation that was missing residues in the fingers domain. We modeled in the missing domain using the complete 4KTQ WT structure. To complete this in silico model, residue 707 of the unblocked WT experimental structure (4KTQ) was modified from an isoleucine to a leucine. This structure was then subjected to 2 μs of MD simulation to account for conformational differences in the fingers domain. Upon simulation convergence, on the basis of RMSD analysis the fingers domain had indeed taken on a conformation similar to that of the 4N56 mutant experimental structure; however, the DNA strand remained in the unblocked position (Figure 2). Preliminarily, this may suggest that the mutant protein favors the blocked state. The coordinates of the fingers region from the in silico I707L mutant were then inserted into the mutant crystal structure (PDB code 4N56) to form a complete mutant binary structure with the DNA strand in the blocked position.

We chose not to use the blocked experimental binary structure of WT *Taq* DNA polymerase (PDB code 3SYZ) because the fingers domain was not resolved in similar regions as the mutant blocked experimental structure (PDB code 4N56). We chose instead to base our initial WT MD structure on the complete mutant binary in silico model described above, which contained a fully resolved fingers domain. To build the WT binary blocked structure, residue 707 in the repaired structure described above was modified in silico from a leucine to an isoleucine, reverting the sequence back to its wild-type counterpart. Further details describing the in silico modeling of the complete structure of the I707L mutant are outlined in Figure S2.

Molecular Dynamics Simulations. All of the simulations (Table 1) were performed using an identical solvation model

Table 1. Summary of Simulations

system/initial structure	T (K)	simulation length (ns)
WT binary blocked	298	1000
WT binary blocked	341	1000
I707L mutant blocked	298	1000
I707L mutant blocked	341	1000

system. The *tleap* module of AmberTools[10] was used to add explicit hydrogen atoms. This was followed by the addition of 33 sodium counterions (Na^+) to neutralize the system. A truncated octahedral unit cell with TIP3P water[11] molecules and a 12.0 Å solvent buffer between the solute and edge of the unit cell resulted in a solvated system count of 82 121 atoms for the mutant and 82 118 atoms for the wild type.

All of the initial structures were minimized, heated, and equilibrated prior to MD. The structures were minimized using a seven-step approach that began with 1000 steps of steepest-descent minimization followed by 4000 steps of conjugate-gradient minimization. The starting positional restraining force of 10.0 kcal mol^{-1} Å^{-1} on the solute heavy atoms[10] was periodically lowered as the system progressed from one step to the next until the last minimization was performed without any restraints.

All of the simulations were heated linearly from 10 K to the desired temperature (298 or 341 K) over 2.0 ns while maintaining 10 kcal mol^{-1} Å^{-1} positional restraints on all heavy atoms of the protein and DNA. Once each simulation reached the desired temperature (298 or 341 K), a 3.5 ns equilibration process was used to reduce the positional restraints in periodic intervals until the final 500 ps of equilibration was performed without restraints.

Unrestrained Molecular Dynamics Simulations. The GPU-accelerated *pmemd* code of Amber 14[10] was used to perform all of the MD steps for every simulation. The Amber *ff12SB* force field[10] was applied to the protein and DNA residues. Unrestrained MD was performed on each simulation at a constant pressure (1 atm) and temperature (298 or 341 K). These parameters were maintained with a Langevin thermostat[12] using periodic boundary conditions. Coordinates, velocities, and energies were saved every 100 ps. The SHAKE algorithm[13] fixed all covalent bond distances involving hydrogen, allowing a 2 fs time step for each simulation. All of the simulations were visualized using VMD v1.9.1,[14] and all analyses were performed with the *cpptraj* module[15] of AmberTools. RMSD and RMSF trajectory plots were aligned to the solvated structure used to initiate the simulations. RMSDs were obtained by alignment to Cα atoms, whereas RMSFs were aligned using all heavy atoms. Welch's unpaired two-sample t test analysis was used to determine the significance between RMSD values obtained from high- and low-temperature simulations.[16]

RESULTS AND DISCUSSION

The purpose of this study was to characterize the dynamics of *Taq* DNA polymerase at low and high temperatures. To do this, MD simulations were used to study the I707L *Taq* DNA polymerase and its wild-type counterpart, WT *Taq* DNA polymerase, at 298 and 341 K.

Unrestrained Molecular Dynamics Results. We performed 1000 ns of MD simulation on each binary complex at 298 and 341 K. We initiated simulations from the blocked forms of the WT and mutant polymerases. These unrestrained simulations did not sample the unblocked conformation, suggesting that a relatively high energy barrier separates the blocked and unblocked conformations. We utilized root-mean-square deviation (RMSD) and root-mean-square fluctuations (RMSF) to define the mobilities of WT and I707L *Taq* DNA polymerase at high and low temperatures.

RMSD Overview. Unrestrained MD suggests that the I707L *Taq* DNA polymerase remained relatively immobile at 298 K and became more flexible at 341 K. This is best illustrated by RMSD values of the movements of the protein relative to the starting structure (Figure 3A). Interestingly, the mutant demonstrated significantly enhanced temperature-dependent mobility relative to the WT. Over the full 1000 ns simulation, the mutant deviated on average 1.71 (±0.04) and 2.14 (±0.08) Å at 298 and 341 K, respectively, whereas the WT average fluctuations were 1.93 (±0.05) Å at 298 K and 1.94 (±0.06) Å at 341 K (values in parentheses report standard deviations of each RMSD data set). To ascertain the significance of these temperature-based differences, we performed an unequal variances (Welch's) two-sample t test on the RMSD ensembles.[16] The t values (Table S1) suggest that the atomic fluctuations for the WT and mutant ensembles are different at each temperature. Temperature-based RMSD differences in the mutant are more significant than in the WT. We also performed the RMSD and t test analysis on a subset of the molecular system, focusing on the O helix and fingers domain (Table S1 and Figure 3C–F). There were no noticeable differences in WT dynamics between the two temperatures (Figure 3B,D,F). On

DOI: 10.1021/acs.jcim.9b00022
J. Chem. Inf. Model. XXXX, XXX, XXX−XXX

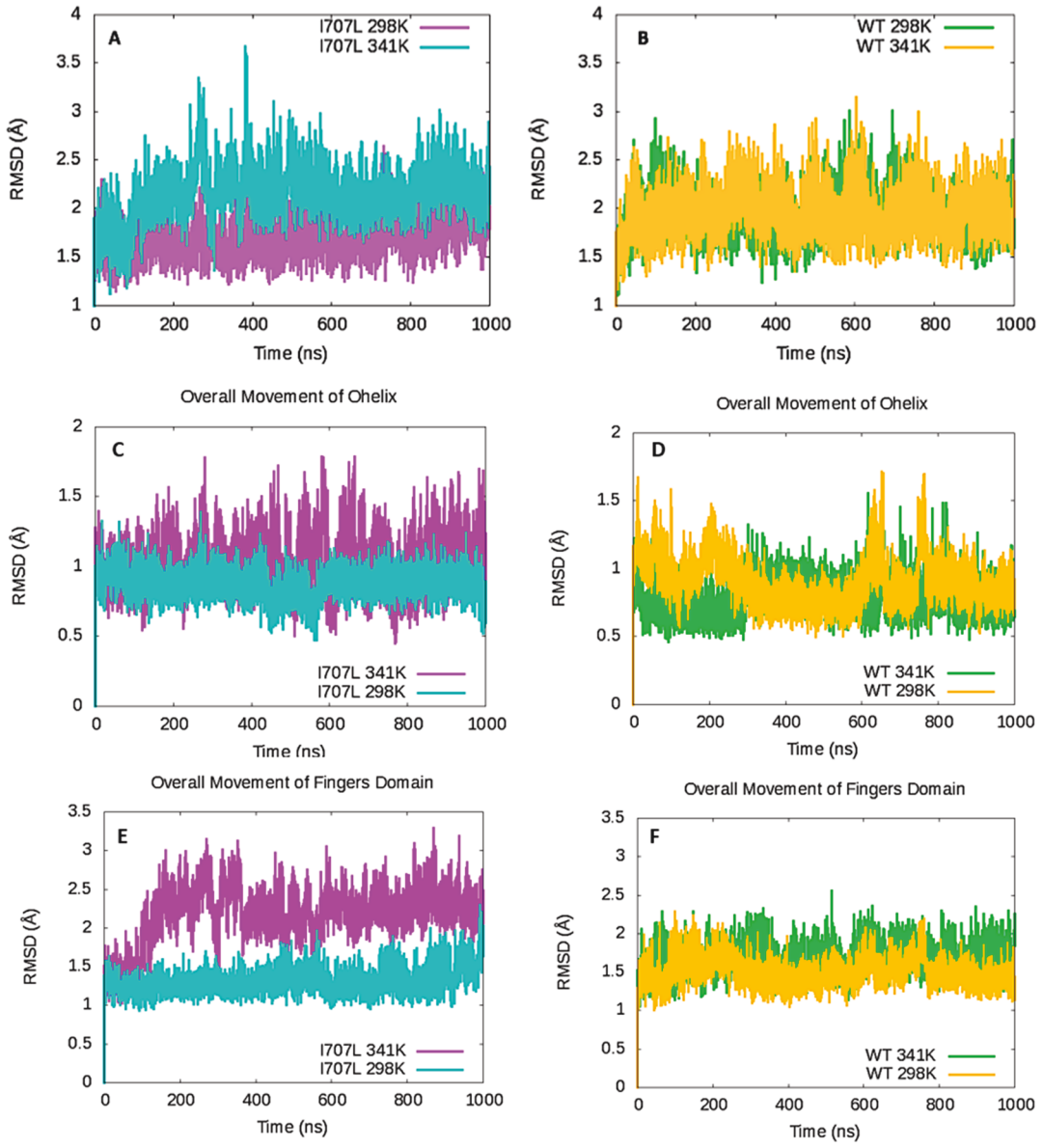

Figure 3. Root-mean-square deviations (RMSDs) over 1000 ns of unrestrained molecular dynamics at 298 and 341 K for (A) I707L *Taq* DNA polymerase and (B) wild-type (WT) *Taq* DNA polymerase. Also shown are RMSD values at 298 and 341 K for the O helix of the (C) I707L mutant and (D) WT as well as for the fingers domain of the (E) mutant and (F) WT.

the basis of these results and our visualization of the resulting ensembles, we would conclude that, as expected, trajectories sampled at higher temperatures show increased mobility. However, the I707L mutant seems better able to undergo larger structural excursions made possible by the higher temperature while remaining structurally intact.

Comparing WT and Mutant Dynamics. The WT motion is characterized by downward movement of the fingers domain and an opening of the active site. This is accompanied by an elongation of the O and O1 helices and a relaxation of the loop region between them (Figure 4B). The I707L mutant presented similar downward movements of the N-terminal end of the O helix, but these motions occurred much earlier in the higher-temperature simulations (Figure 4C). At the higher temperature, the mutant also exhibited elongation of the Q helix, and this created extra space into which the loop region between the O and O1 helices moved.

Comparing High- and Low-Temperature Behavior. We also compared the dynamical behaviors of the WT polymerase at high and low temperatures and the mutant polymerase at both temperatures (Figure S3). At 298 K, the WT is more mobile (has a higher average RMSD (1.93 Å)) than the mutant polymerase (average RMSD = 1.71 Å) (Figure S3A). Visualization of the lower-temperature trajectories at ∼600 ns revealed that the O1 helix and the tip of the fingers domain of WT *Taq* DNA polymerase rest higher up in the active site than the same helices in the I707L *Taq* DNA polymerase structure (Figure S4B). The Q helix of I707L *Taq* DNA polymerase lies slightly higher in the active site than that of WT *Taq* DNA polymerase (Figure S4B). The top of the thumb domain of WT *Taq* DNA polymerase sits further away from the active site than its I707L counterpart (Figure S4A), further characterizing the differences between the mutant and WT at low temperature. The decreased mobility of the mutant at low temperature (Figure S3A) suggests that the

DOI: 10.1021/acs.jcim.9b00022
J. Chem. Inf. Model. XXXX, XXX, XXX−XXX

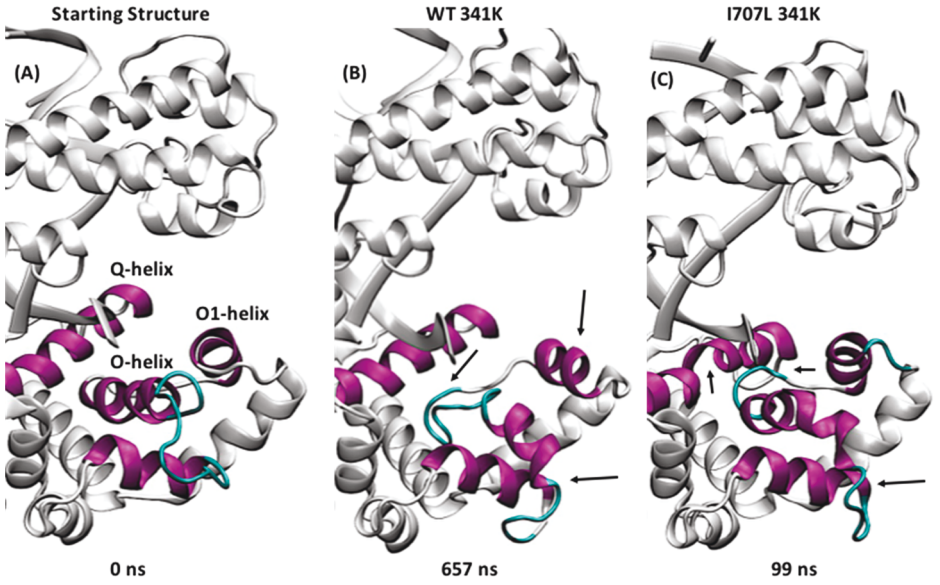

Figure 4. Illustration of the polymerase dynamics at 341 K for both I707L and WT *Taq* DNA polymerase. At this temperature, there are increased flexibility in the N-terminal ends of the Q and O helices and increased movements in the loop between the O and O1 helices. The colored areas highlight these dynamic regions. (A) Illustration of the starting structure of the protein. (B) Illustration of the movements that resulted in the RMSD shift seen at 657 ns for WT *Taq* DNA polymerase. (C) Illustration of the movements responsible for the RMSD peak at around 100 ns for I707L Taq DNA polymerase.

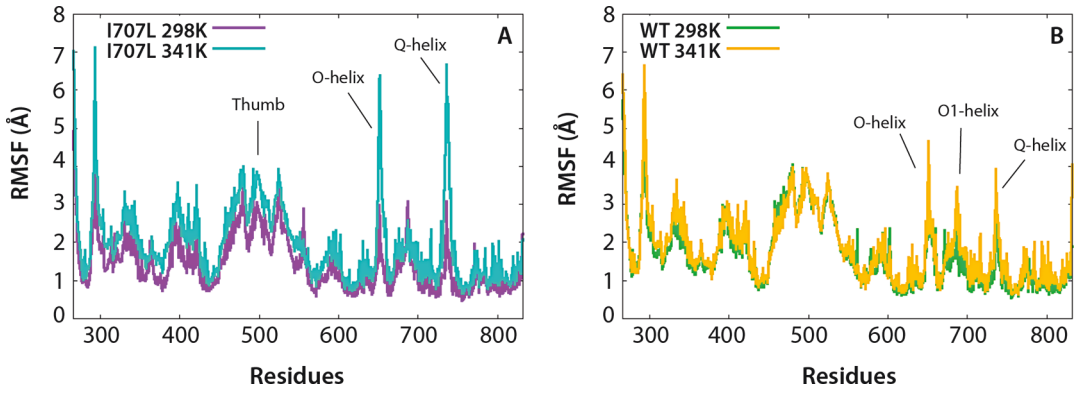

Figure 5. Root-mean-square fluctuations (RMSF) of each residue in *Taq* DNA polymerase after 1000 ns at 298 and 341 K. (A) The most mobile residues of the I707L mutant at 341 K were at the N-terminal ends of the O and Q helices. (B) Such a significant temperature-dependent difference in residue movements was not seen for the WT *Taq* DNA polymerase. The thumb domain, however, appears to be more dynamic at 341 K.

mutant remains longer in the blocked conformation, which may lead to reduced activity relative to the WT at 298 K.

RMSF Analysis. To understand the dynamical differences between mutant and WT *Taq* DNA polymerase at low and high temperature, we also examined residue fluctuations (root-mean-square fluctuations, RMSF). The most notable differences in mobility in the mutant as a function of temperature occurred at the N-terminal ends of the O and Q helices (Figure 5A). At low temperature, residues in these helices move approximately 3 Å, whereas at high temperature the O and Q helices make excursions of up to 6.8 and 7.5 Å. The WT does display some temperature-dependent mobility, particularly in the O and O1 helices. The residues fluctuate up to 4.5 Å, suggesting that this region is not as mobile as in the mutant. The WT Q helix is a bit more mobile at higher temperatures but again not as mobile as in the mutant at 341 K (Figure 5B). At high temperatures, the O and Q helices in the mutant are substantially more mobile than those in the WT at either temperature. We investigated the differences in mobility of the disordered regions (~643−660 and ~670−699) as suggested by the experimental *B*-factors. RMSF plots of these regions (Figure S5) show that there is significantly more fluctuation in the region corresponding to residues 643−660 in the mutant at high temperature than in the mutant at low temperature and the WT at either temperature. In addition, we examined the fluctuations of residues mutated in other studies/structures (626, 706, and 708) and found that residue 626 (Glu626) had similar fluctuations in the mutant at both temperatures while in the WT this residue was more mobile at high temperature. For residues 706 and 708 more mobility was observed at higher temperatures for both the WT and mutant. Detailed images of the RMSF plots in these regions can be found in Figure S5.

Principal Component Analysis. Principal component analysis (PCA) was also used to extract the dominant structural movements of the mutant and WT during the 1000 ns of unrestrained simulation at high and low temperature. The top four modes captured 40−50% of the polymerase motion (Table S2). The fifth and higher modes contributed less than 5% each,

DOI: 10.1021/acs.jcim.9b00022
J. Chem. Inf. Model. XXXX, XXX, XXX−XXX

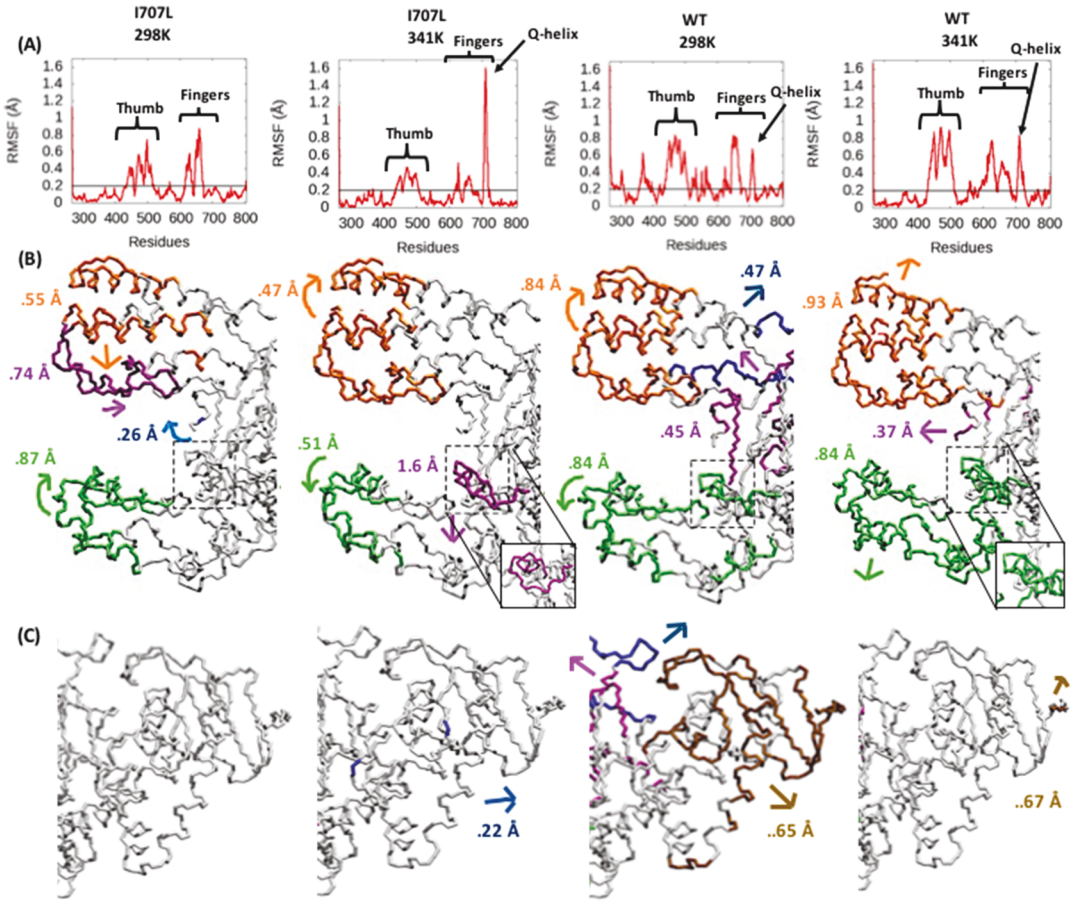

Figure 6. First principal components of the WT and mutant simulations at high and low temperatures. The distance values shown above are indicative of the RMSF of the residue that deviated the farthest. (A) RMSF of the most prominent modes of movement. The horizontal black lines at 0.2 Å indicate the RMSF cutoff used to define significant motion. (B) Directional movements of residues that moved on average more than 0.2 Å in the forefront of the *Taq* DNA polymerase are shown with arrows. Residues that moved synchronously are indicated with the same color. The dotted box marks the initial location of the Q helix. The solid box indicates the final position of the Q helix. (C) Directional movements of residues that moved on average more than 0.2 Å on the back end of the polymerase. The DNA strand is not shown, as the PCA analysis focused on protein α-carbon atoms.

and the RMSF for higher-order modes had fewer residues with deviations above the 0.2 Å threshold. Eigenvectors corresponding to the top three principal components were saved as pseudotrajectory files that were visualized and used for subsequent RMSF analysis. The RMSF data allowed us to characterize the major motions associated with each of the three most significantly weighted eigenvectors for each simulation. Visualizations of the top two modes are shown in Figures 6A and 7A. We defined a cutoff of 0.2 Å above which significant residue fluctuation occurred, and we inspected these regions closely.

In the most significant (heavily weighted) principal component of I707L *Taq* DNA polymerase, the Q helix experienced major fluctuations (1.6 Å) at 341 K; however, at 298 K the Q helix was less dynamic (Figure 6A,B). Additionally, the most prevalent movements of the mutant polymerase at 298 K consisted of the finger and thumb domains moving toward each other, closing the active-site cleft, while at 341 K the two domains swiveled away from each other, opening the active site. This suggests that at the higher temperature the polymerase opens, allowing the DNA to transition from the blocked position to the unblocked position, while at lower temperature the polymerase prevents such conformational change by closing around the DNA and keeping it in the blocked position. For WT *Taq* DNA polymerase at 298 K, PCA revealed significant movements throughout the protein including the thumb and fingers domain (Figure 6B,C). As the fingers and thumb domains swivel away from each other in opposite directions, the back end of the protein moves downward (Figure 6C). At 341 K, there were similar outward directional movements by the fingers and thumb domains, but we observed little corresponding movement in the back of the protein. Interestingly, the motion of the fingers domain and Q helix are decoupled in the mutant but coupled in the WT, i.e., for the WT the fingers domain and the Q helix moved simultaneously and directionally downward at both temperatures, but for the mutant these motions occurred independently (Figure 6B).

While the modes of motion for the second principal component are different from the first, this mode also shows the opening of the WT active site. As in the first mode, the Q helix motion is most significant in the high temperature mutant simulation and is again decoupled from the fingers domain in the mutant at 341 K but coupled in the WT at 298 and 341 K (Figure 7). At both temperatures, the WT fingers and thumb domains moved outward, opening the active site, whereas in the mutant at both temperatures the fingers and thumb domains move to close the active site (Figure 7B). For the mutant at 341 K, the Q helix movements were decoupled from the movements of the fingers domain. The Q helix moved downward as the rest of the fingers domain moved upward, while at 298 K the Q helix remained immobile as the rest of the fingers domain moved up.

DOI: 10.1021/acs.jcim.9b00022
J. Chem. Inf. Model. XXXX, XXX, XXX−XXX

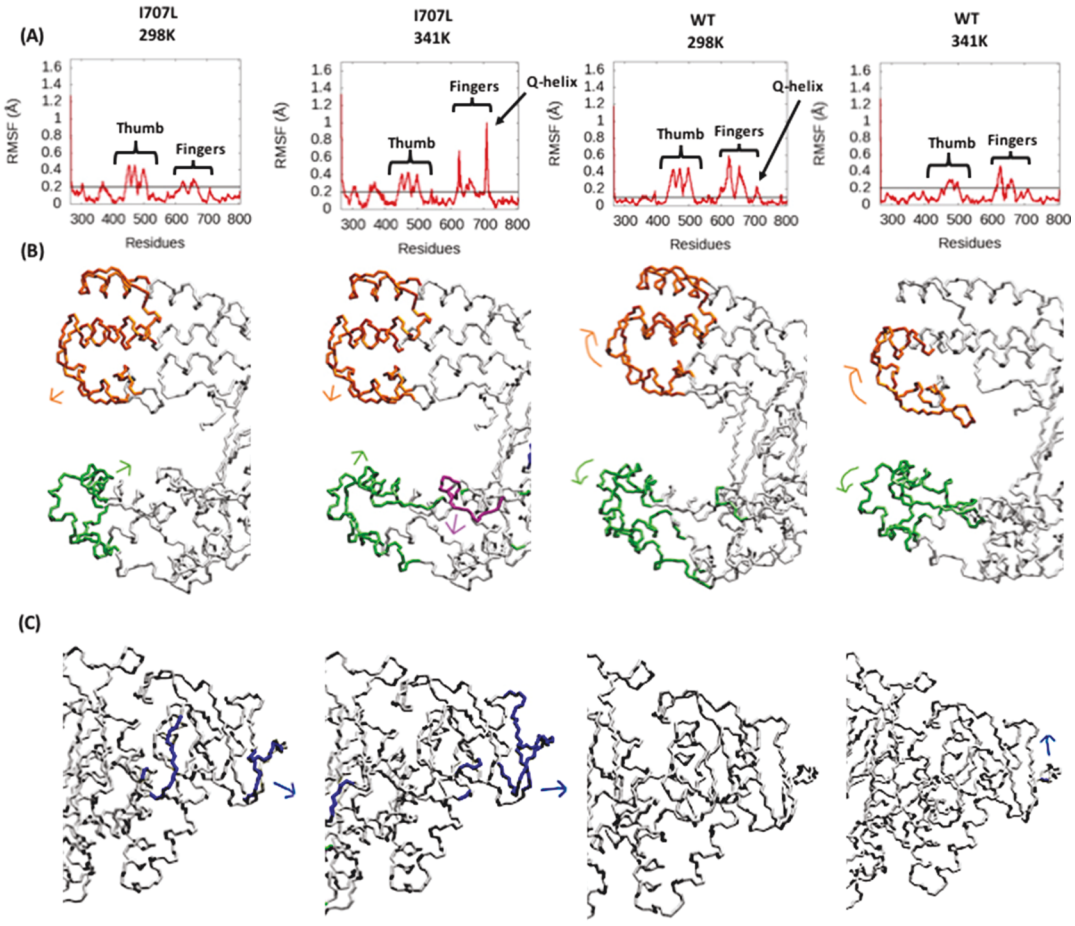

Figure 7. Second principal component. (A) RMSF of the second highest mode of movement. The horizontal black lines 0.2 Å indicate the RMSF cutoff used to define significant motion.(B) Directional movements of residues that moved on average more than 0.2 Å in the forefront of the Taq DNA polymerase. (C) Directional movements of residues that moved on average more than 0.2 Å on the back end of *Taq* DNA polymerase. Residues that moved synchronously are indicated with the same color. The DNA strand is not shown, as the PCA analysis focused on protein α-carbon atoms.

Movement in the back of the protein was seen only with the I707L *Taq* DNA polymerase (Figure 7C).

In the third principal component, the fingers domain of the WT remains mobile at both temperatures, whereas the thumb domain moves mostly at 298 K. This is the first mode of motion where the WT fingers and thumb domain move inward, closing the active-site cleft. For the mutant at lower temperature, only the tip of the fingers domain is mobile and moving upward toward the active site. At 341 K, the mutant O helix and fingers domain remain very mobile, moving downward to open the cleft.

We have projected the top two PCA modes from each of the four simulations onto the same eigenspace (Figure 8A). This demonstrates that the major motions for the high-temperature I707L mutant are different from the motions of the other simulations and that the greatest difference in movement is generated mainly by residues in the O and Q helices. These plots further demonstrate the temperature sensitivity of the mutant. We also plotted modes 1 and 2 for the mutant and WT (Figure 8B), showing that the high-temperature motion of the mutant is dominated by two distinct states not seen in the other dynamical analyses. The projection of modes 2 and 3 did not show such distinctions (Figure S6). All of the projection plots show densely populated areas suggestive of well-sampled simulations.

In the original paper that described the I707L cold-sensitive mutations,[3] there were three other mutations that also resulted in sensitivity to cold (E626K, W706R, and E708D.) Visualization of the trajectories and RMSF plots generated in this study did not reveal any unusual temperature-dependent conformational behavior on the part of these residues. We have also examined the trajectories for structural and/or energetic interactions with residues within 3 Å of I707 and L707 (Table S3). An MM-GBSA analysis of residues interacting with I707 and L707 did not reveal any significant interactions. A per-residue decomposition analysis did reveal groups of residues *near* I707 and L707 that contribute significantly to the overall MM-GBSA energy. These residues may be interesting candidates for experimental mutation (Figure S7).

It has previously been shown that the I707L mutation results in a functionally slower polymerase at lower temperature. However, the mechanism for the change in function was not known. The long simulations used in this study have allowed us to understand how a single-point mutation alters the domain movement and functionality of the polymerase. The RMSD, RMSF, and PCA results suggest that this single-point mutation results in a mutant that is mechanistically different and substantially less mobile at lower temperatures. Our RMSD and RMSF calculations yielded results consistent with the experimental picture in that the overall mobility of the polymerase is greater at higher temperatures. This gives us confidence in the accuracy of our ensembles and validates the physical picture that emerges from the PCA analysis. Our results indicate that the mutant is less mobile at low temperature

DOI: 10.1021/acs.jcim.9b00022
J. Chem. Inf. Model. XXXX, XXX, XXX−XXX

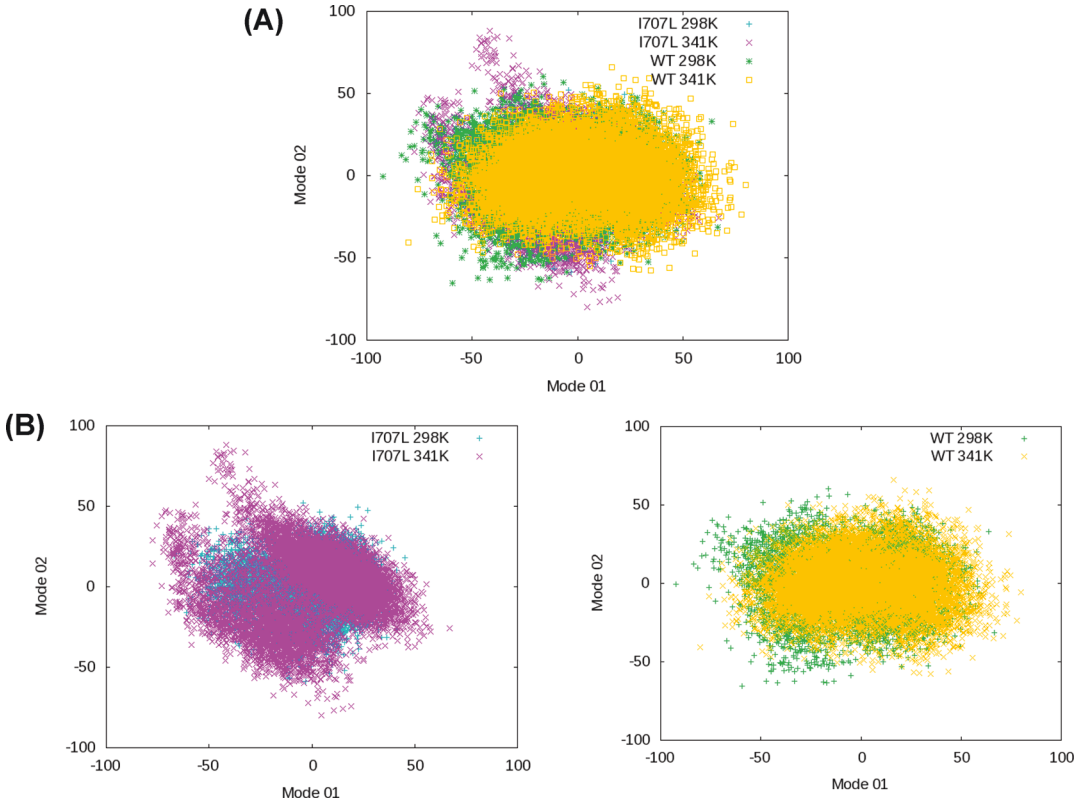

Figure 8. Projections of PCA modes 1 and 2. (A) Consensus projection of each of the four simulations onto the same eigenspace. (B) Mode 1 vs mode 2 projections for (left) the mutant and (right) the WT.

relative to the WT at both temperatures and the mutant at high temperatures. Furthermore, our results show that the I707L mutation results in a structural decoupling of the Q helix from the fingers domain, leading to a temperature dependence of the movement of the Q helix, which is more flexible at high temperature and less flexible at low temperature. PCA analysis of the resulting MD ensemble also suggests that the I707L mutation results in a polymerase that is more likely to close at low temperature, whereas the WT and high-temperature polymerase motion is dominated by opening of the active site. To assess dynamical coupling, we used the AMBER module *cpptraj* to generate dynamic cross-correlation maps for the WT and mutant simulations at low and high temperature (Figure S8).[17] Correlation maps are $N \times N$ heat maps, where N is the number of α-carbons in the molecule. Each element in the heat map corresponds to dynamic coupling between each pair of atoms i, j. These plots help to identify regions of the molecule that move synchronously (red) or independently (blue). We can see from this dynamical analysis that the Q helix and the fingers domain are most negatively correlated (decoupled) in the WT at 298 K. The decoupling seen in the PCA analysis is a structural decoupling where the tip of the Q helix moves independently from the fingers domain but in the same direction. In the dynamic correlation maps we see independent motions (most prominent in the WT at low temperature) in which the residues move in opposite directions. It is important to note that the residues shown to be most negatively dynamically correlated are different residues than those shown in the PCA analysis, i.e., these residues are not in the tip of the Q helix. Taken together, these results suggest reduced mobility of the mutant at low temperature, perhaps keeping it in the blocked position for longer periods of time, leading to reduced activity. It is our hope that this atomistic understanding and comparison of the mutant and WT polymerase can be used in future mutational studies to further improve the function of the polymerase.

CONCLUSIONS

We have identified key characteristics of the dynamics of *Taq* DNA polymerase at low and high temperatures. Unrestrained MD revealed substantially more movement in the mutant *Taq* DNA polymerase at high temperature, especially in the N-terminal ends of the Q and O helices. These results support the notion that the I707L mutation, while occurring in the P helix some distance away from the active site, exerts influence on the dynamics near the active site. Our results also find that this effect is temperature-dependent: the Q helix in particular is more mobile in the mutant at high temperatures, whereas the lower-temperature mutant simulations were similar to the WT trajectories at both low and high temperature. Our simulations also provide a more nuanced explanation for the relatively slow activity of the I707L mutant at low temperature. Our results suggest that when the mutant polymerase active site is blocked, it stays blocked longer because of the reduced dynamics at low temperature (Figure 3), but when the temperature is elevated, increased movements in the O and Q helices (Figure 5A) may allow the polymerase to escape the blockage. Principal component analysis revealed that for the mutant at high temperatures, the motion of the Q helix was decoupled from the dynamics of the fingers domain (Figure 6B). This structural decoupling was not observed for the WT at either temperature nor for the mutant simulation at low temperature. In those cases, the Q helix moved in concert with the fingers domain. In addition to this, the PCA results show that at the lower temperature the mutant is more likely to undergo a closing

DOI: 10.1021/acs.jcim.9b00022
J. Chem. Inf. Model. XXXX, XXX, XXX−XXX

motion, while at the increased temperature the mutant prefers the opening motion.

■ ASSOCIATED CONTENT

Supporting Information

The Supporting Information is available free of charge on the ACS Publications website at DOI: 10.1021/acs.jcim.9b00022.

Electrostatic surface maps comparing the F749 conformations in the WT and mutant experimental structures, additional details on the construction of the initial models, a comparison of the simulation trajectories at the same temperature, a close-up schematic of mutant and WT structural differences, RMSF details for residues 640−660, PCA details, correlation maps, and *t*-test results (PDF)

■ AUTHOR INFORMATION

Corresponding Author

*Address: Department of Chemistry, Gottwald Center for the Sciences, University of Richmond, 28 Westhampton Way, Richmond, VA 23173. E-mail: cparish@richmond.edu.

ORCID

Carol A. Parish: 0000-0003-2878-3070

Notes

The authors declare no competing financial interest.

■ ACKNOWLEDGMENTS

This research was supported by the Jeffress Trust Awards Program in Interdisciplinary Research (E.W. and C.A.P.), the NSF RUI Program (Grants CHE-1213271 and CHE-1800014 to C.A.P.), and the Donors of the American Chemical Society Petroleum Research Fund (C.A.P.). Computational resources were provided in part by the MERCURY supercomputer consortium under NSF Grant CHE-1626238. E.M. and L.M. acknowledge support from the University of Richmond Arts and Sciences Undergraduate Research Committee.

■ REFERENCES

(1) Saiki, R. K.; Gelfand, D. H.; Stoffel, S.; Scharf, S. J.; Higuchi, R.; Horn, G. T.; Mullis, K. B.; Erlich, H. A. Primer-Directed Enzymatic Amplification of DNA with a Thermostable DNA Polymerase. *Science* **1988**, *239*, 487−91.

(2) Chou, Q.; Russell, M.; Birch, D. E.; Raymond, J.; Bloch, W. Prevention of Pre-Pcr Mis-Priming and Primer Dimerization Improves Low-Copy-Number Amplifications. *Nucleic Acids Res.* **1992**, *20*, 1717−23.

(3) Kermekchiev, M. B.; Tzekov, A.; Barnes, W. M. Cold-Sensitive Mutants of Taq DNA Polymerase Provide a Hot Start for Pcr. *Nucleic Acids Res.* **2003**, *31*, 6139−47.

(4) Wu, E. Y.; Walsh, A. R.; Materne, E. C.; Hiltner, E. P.; Zielinski, B.; Miller, B. R., 3rd; Mawby, L.; Modeste, E.; Parish, C. A.; Barnes, W. M.; et al. A Conservative Isoleucine to Leucine Mutation Causes Major Rearrangements and Cold Sensitivity in Klentaq1 DNA Polymerase. *Biochemistry* **2015**, *54*, 881−9.

(5) Ollis, D. L.; Brick, P.; Hamlin, R.; Xuong, N. G.; Steitz, T. A. Structure of Large Fragment of Escherichia Coli DNA Polymerase I Complexed with Dtmp. *Nature* **1985**, *313*, 762−6.

(6) Li, Y.; Korolev, S.; Waksman, G. Crystal Structures of Open and Closed Forms of Binary and Ternary Complexes of the Large Fragment of Thermus Aquaticus DNA Polymerase I: Structural Basis for Nucleotide Incorporation. *EMBO J.* **1998**, *17*, 7514−25.

(7) Betz, K.; Malyshev, D. A.; Lavergne, T.; Welte, W.; Diederichs, K.; Dwyer, T. J.; Ordoukhanian, P.; Romesberg, F. E.; Marx, A. Klentaq Polymerase Replicates Unnatural Base Pairs by Inducing a Watson-Crick Geometry. *Nat. Chem. Biol.* **2012**, *8*, 612−4.

(8) Miller, B. R., 3rd; Parish, C. A.; Wu, E. Y. Molecular Dynamics Study of the Opening Mechanism for DNA Polymerase I. *PLoS Comput. Biol.* **2014**, *10*, No. e1003961.

(9) Dyson, H. J. Roles of Intrinsic Disorder in Protein-Nucleic Acid Interactions. *Mol. BioSyst.* **2012**, *8*, 97−104.

(10) Case, D. A.; Babin, V.; Berryman, J. T.; Betz, R. M.; Cai, Q.; Cerutti, D. S.; Cheatham, T. E., III; Darden, T. A.; Duke, R. E.; Gohlke, H.; Goetz, A. W.; Gusarov, S.; Homeyer, N.; Janowski, P.; Kaus, J.; Kolossváry, I.; Kovalenko, A.; Lee, T. S.; LeGrand, S.; Luchko, T.; Luo, R.; Madej, B.; Merz, K. M.; Paesani, F.; Roe, D. R.; Roitberg, A.; Sagui, C.; Salomon-Ferrer, R.; Seabra, G.; Simmerling, C. L.; Smith, W.; Swails, J.; Walker, R. C.; Wang, J.; Wolf, R. M.; Wu, X.; Kollman, P. A. *Amber 14*; University of California, San Francisco, 2014.

(11) Jorgensen, W. L.; Madura, J. D. Quantum and Statistical Studies of Liquids 0.25. Solvation and Conformation of Methanol in Water. *J. Am. Chem. Soc.* **1983**, *105*, 1407−1413.

(12) Zwanzig, R. Nonlinear Generalized Langevin Equations. *J. Stat. Phys.* **1973**, *9*, 215−220.

(13) Ryckaert, J. P.; Ciccotti, G.; Berendsen, H. J. C. Numerical-Integration of Cartesian Equations of Motion of a System with Constraints - Molecular-Dynamics of N-Alkanes. *J. Comput. Phys.* **1977**, *23*, 327−341.

(14) Humphrey, W.; Dalke, A.; Schulten, K. VMD: Visual Molecular Dynamics. *J. Mol. Graphics* **1996**, *14*, 33−8.

(15) Roe, D. R.; Cheatham, T. E., III. Ptraj and Cpptraj: Software for Processing and Analysis of Molecular Dynamics Trajectory Data. *J. Chem. Theory Comput.* **2013**, *9*, 3084−95.

(16) Ruxton, G. D. The Unequal Variance T-Test Is an Underused Alternative to Student's T-Test and the Mann−Whitney U Test. *Behav. Ecol.* **2006**, *17*, 688−690.

(17) Kasahara, K.; Fukuda, I.; Nakamura, H. A Novel Approach of Dynamic Cross Correlation Analysis on Molecular Dynamics Simulations and Its Application to Ets1 Dimer−DNA Complex. *PLoS One* **2014**, *9*, No. e112419.

DOI: 10.1021/acs.jcim.9b00022
J. Chem. Inf. Model. XXXX, XXX, XXX−XXX